1521-009X/49/10/910–918$35.00
DRUG METABOLISM AND DISPOSITION
Copyright © 2021 by The American Society for Pharmacology and Experimental Therapeutics
https://doi.org/10.1124/dmd.121.000505
Drug Metab Dispos 49:910–918, October 2021

Tetrahydrocannabinol and Its Major Metabolites Are Not (or Are Poor) Substrates or Inhibitors of Human P-Glycoprotein [ATP-Binding Cassette (ABC) B1] and Breast Cancer Resistance Protein (ABCG2)

Xin Chen, Jashvant D. Unadkat, and Qingcheng Mao

Department of Pharmaceutics, School of Pharmacy, University of Washington, Seattle, Washington

Received April 16, 2021; accepted July 13, 2021

ABSTRACT

(−)-Δ^9-Tetrahydrocannabinol (THC) is the primary psychoactive constituent of cannabis. In humans, 11-hydroxy-THC (11-OH-THC) and 11-nor-9-carboxy-THC (THC-COOH) are psychoactive and nonpsychoactive circulating metabolites of THC, respectively. Whether these cannabinoids are substrates or inhibitors of human P-glycoprotein (P-gp) or breast cancer resistance protein (BCRP) is unknown. Previous animal studies suggest that THC and its metabolites could be substrates of these transporters. Therefore, we performed Transwell, cellular accumulation, and vesicular transport assays, at pharmacologically relevant concentrations of these cannabinoids, using Madin-Darby canine kidney (MDCK) II cells or plasma membrane vesicles overexpressing human P-gp or BCRP. Neither THC nor 11-OH-THC was found to be a substrate or inhibitor of P-gp or BCRP. The efflux ratio of THC-COOH in MDCKII-BCRP cells was 1.6, which was significantly decreased to 1.0 by the BCRP inhibitor Ko143. Likewise, cellular accumulation of THC-COOH was significantly increased 1.6-fold in the presence versus absence of Ko143. THC-COOH also significantly inhibited BCRP-mediated transport of Lucifer yellow, a BCRP substrate; however, THC-COOH was neither a substrate nor an inhibitor of P-gp. Collectively, these results indicate that THC and 11-OH-THC are not substrates or inhibitors (at pharmacologically relevant concentrations) of either P-gp or BCRP. THC-COOH is a weak substrate and inhibitor of BCRP, but not of P-gp. Accordingly, we predict that P-gp/BCRP will not modulate the disposition of these cannabinoids in humans. In addition, use of these cannabinoids will not result in P-gp– or BCRP-based drug interactions.

SIGNIFICANCE STATEMENT

This study systematically investigated whether Δ^9-tetrahydrocannabinol (THC) and its major metabolites, 11-hydroxy-THC and 11-nor-9-carboxy-THC, are substrates and/or inhibitors of human P-gp and BCRP at pharmacologically relevant concentrations. The results obtained are highly valuable for mechanistic understanding and prediction of the roles of P-gp and BCRP in determining the human pharmacokinetics, tissue distribution, and drug interactions of cannabinoids.

Introduction

Cannabinoids are chemicals found in cannabis with diterpene structure (Booth and Bohlmann, 2019). Among over 100 well characterized cannabinoids, (−)-Δ^9-tetrahydrocannabinol (THC) is the principal psychoactive constituent of cannabis, and it can be sequentially metabolized primarily by the cytochrome P450 enzyme CYP2C9 to the psychoactive 11-hydroxy-THC (11-OH-THC) and then to the nonactive 11-nor-9-carboxy-THC (THC-COOH) (Grotenhermen, 2003; Patilea-Vrana and Unadkat, 2019). Cannabis use is increasing in the United States (Carliner et al., 2017). Although cannabis is widely used, oral synthetic THC (dronabinol) is a Food and Drug Administration–approved drug for the treatment of nausea, vomiting, and anorexia (Schwilke et al., 2009). As such, it is necessary to understand the mechanisms by which the disposition of THC and its metabolites is mediated. Although the disposition of THC and its major metabolites via drug-metabolizing enzymes such as the cytochrome P450 enzymes has been extensively studied (Stout and Cimino, 2014; Patilea-Vrana et al., 2019; Patilea-Vrana and Unadkat, 2019; Qian et al., 2019), very little information is available about the roles of drug transporters in the disposition of these cannabinoids.

P-glycoprotein (P-gp) is a member of the ATP-binding cassette (ABC) efflux transporter family encoded by the gene *ABCB1* (Ueda et al., 1987). P-gp is expressed throughout the human body, with particularly high expression at the blood-brain barrier, the placental syncytiotrophoblast, the intestinal epithelium, the liver bile canaliculi, and kidney proximal tubular epithelium (Hodges, 2011). Many structurally and chemically unrelated compounds are found to be P-gp substrates (Hodges, 2011). Its broad substrate specificity and high expression in organs important for drug disposition renders P-gp a critical role in determining drug pharmacokinetics, efficacy, or toxicity. Breast cancer

This work was supported by National Institutes of Health National Institute on Drug Abuse [Grant P01DA032507].

The authors declare no conflict of interest.

http://dx.doi.org/10.1124/dmd.121.000505.

ABBREVIATIONS: A→B, apical to basolateral; ABC, ATP-binding cassette; ACN, acetonitrile; AUC, area under concentration-time curve; B→A, basolateral to apical; BCRP, breast cancer resistance protein; DMEM, Dulbecco's modified Eagle's medium; ER, efflux ratio; HBSS, Hank's balanced salt solution; Ko143, (3*S*,6*S*,12aS)-1,2,3,4,6,7,12,12a-octahydro-9-methoxy-6-(2-methylpropyl)-1,4-dioxopyrazino[1',2':1,6]pyrido[3,4-b]indole-3-propanoic acid 1,1-dimethylethyl ester; LC-MS/MS, liquid chromatography–tandem mass spectrometry; LY, Lucifer yellow; m/z, mass to charge ratio; MDCK, Madin-Darby canine kidney; NMQ, *N*-methyl-quinidine; 11-OH-THC, 11-hydroxy-Δ^9-tetrahydrocannabinol; P_{app}, apparent permeability; P-gp, P-glycoprotein; THC, (−)-Δ^9-tetrahydrocannabinol; THC-COOH, 11-nor-9-carboxy-Δ^9-tetrahydrocannabinol.

Downloaded from dmd.aspetjournals.org at ASPET Journals on October 14, 2022

resistance protein (BCRP) encoded by the gene *ABCG2* is another vital member of the ABC transporter family (Allikmets et al., 1998; Doyle et al., 1998; Miyake et al., 1999). The pattern of tissue distribution and expression of BCRP highly resembles that of P-gp (Maliepaard et al., 2001; Aronica et al., 2005; Fetsch et al., 2006). Like P-gp, BCRP has a very broad spectrum of substrates, ranging from hydrophobic anticancer drugs to hydrophilic conjugate organic anions (Mao and Unadkat, 2015). Therefore, BCRP also plays a critical role in the disposition of many drugs and xenobiotics (Safar et al., 2019).

Regarding the roles of P-gp and BCRP in the disposition of cannabinoids, Bonhomme-Faivre et al. (2008) reported that the area under concentration-time curve (AUC) of THC (administered orally) in *P-gp*–deficient CF1 mice was 2.17-fold higher than that in wild-type CF1 mice, suggesting that the mouse P-gp could limit oral absorption. Another study using *P-gp* and *Bcrp* knock-out mice showed that the brain/blood THC ratios are higher than those in wild-type mice at certain time points after intraperitoneal administration (Spiro et al., 2012). In addition, *P-gp* and *Bcrp* knock-out mice are more sensitive to THC-induced hypothermia (Spiro et al., 2012). These data suggest that THC is a substrate of mouse P-gp and Bcrp. Furthermore, a study using pregnant macaque revealed that, after THC intravenous administration, fetal THC AUC is ∼30% of maternal THC AUC, and fetal exposure of THC-COOH is undetectable (Bailey et al., 1987). These data suggest that P-gp and/or BCRP, highly expressed on the apical membrane of the placental syncytiotrophoblasts of the macaques, may limit fetal exposure to THC and THC-COOH by transporting these cannabinoids back to the maternal circulation. THC has been shown to be a weak inhibitor of human P-gp via *in vitro* inhibition studies using a rather high, not pharmacologically relevant concentration (50 μM) (Tournier et al., 2010). To date, no *in vitro* transport studies have been reported to show that THC and any of its metabolites, at pharmacologically relevant concentrations, are substrates and/or inhibitors of human P-gp and BCRP. In this study, we systematically investigated whether THC, 11-OH-THC, or THC-COOH, at pharmacologically relevant concentrations, are substrates and/or inhibitors of human P-gp and BCRP.

Materials and Methods

(−)-Δ^9-THC (50 mg/mL) and d^8-loperamide were purchased from Cayman Chemicals (Ann Arbor, MI). (±)11-OH-THC (100 μg/mL), (±)11-nor-9-carboxy-THC (THC-COOH) (1 mg/mL), (−)-Δ^9-d^3-THC, and (±)-d^3-11-OH-THC in methanol were purchased from Cerilliant (Round Rock, TX). Bovine serum albumin Fraction V, *N*-methyl-quinidine (NMQ), Ko143, ATP, AMP, and prazosin were from Sigma-Aldrich (St. Louis, MO). Tris, HEPES, 0.25% trypsin-EDTA, geneticin, GlutaMAX, Dulbecco's phosphate-buffered saline, Hank's balanced salt solution (HBSS) (with Ca^{2+}), FBS, Dulbecco's modified Eagle's medium (DMEM) (4.5 g/L glucose and 1.0 g/L glucose), acetonitrile (ACN), DMSO, and formic acid (liquid chromatography–mass spectrometry–grade) were from Thermo Fisher Scientific (Hampton, NH). Multiscreen HTS Vacuum Manifold, 96-well FC Filter Plates [1.2/0.65 μm, opaque, nonsterile (MSFCN6B10)] were purchased from EMD Millipore (Billerica, MA). Tariquidar was obtained from AzaTrius Pharmaceuticals Private Limited, India. Lucifer yellow (LY) was from MP Biomedicals (Irvine, CA). Hygromycin B, 24-well cell culture plate, and 12-well Transwell plate were from Corning (Corning, NY). The bicinchoninic acid assay protein quantification kit was from Pierce Chemical (Rockford, IL). SB MDR1/P-gp HEK293 and SB BCRP HEK293 plasma membrane vesicles (5 mg/mL) overexpressing human P-gp and BCRP, respectively, were obtained from SOLVO Biotechnology (Szeged, Hungary). Low-binding microcentrifuge tubes were from Genesee Scientific (San Diego, CA). Milli-Q water was used in all preparations. All other chemicals and reagents were obtained at the highest quality available commercially.

Cell Culture. MDCKII-hMDR1-cMDR1-KO (MDCKII-P-gp) cells were a kind gift from Dr. Per Artursson, Uppsala University, Sweden, and MDCKII-BCRP cells were developed in the laboratory of Dr. Qingcheng Mao by stable transfection of the pcDNA-BCRP plasmid into MDCKII cells. All cells were preserved in liquid N_2. The passages of MDCKII cells used in Transwell and cellular accumulation assays ranged from the 1st to 10th passages. We adopted culture conditions established in respective laboratories for both cell lines—namely, MDCKII-P-gp cells were cultured in high-glucose (4.5 g/L) DMEM supplemented with 10% FBS, 1% GlutaMAX, 1% penicillin-streptomycin, and 375 μg/mL hygromycin B, and MDCKII-BCRP cells were cultured in low-glucose (1.0 g/L) DMEM with 10% FBS, 1% penicillin-streptomycin, and 500 μg/mL geneticin. All cells were maintained in a humidified incubator at 37°C in 5% CO_2 with 95% humidity. When reaching ∼90% confluency, cells were passed into a new flask after washing with Dulbecco's phosphate-buffered saline and trypsinization and were then seeded into Transwell inserts or 24-well plates for subsequent transport assays (see below). In MDCKII-P-gp cells, the canine P-gp/ABCB1 gene has been knocked out (Karlgren et al., 2017), whereas in MDCKII-BCRP cells, the canine BCRP/ABCG2 gene is not knocked out. However, parent MDCKII cells do not express canine BCRP protein or possess transport activity of canine BCRP (Tournier et al., 2010).

Bidirectional Transwell Transport Assay. MDCKII cells expressing human P-gp or BCRP were seeded onto Collagen I–coated Transwell plates with a density of approximately 5×10^5 cells per well and cultured for 4 days to form tight junctions. On the day of the assay, the transepithelial/endothelial electrical resistance was measured to be at least 180 Ω. Each apical chamber was washed three times with 0.5 mL of HBSS (with Ca^{2+} and supplemented with 10 mM HEPES for all experiments unless specified), and each basolateral chamber was washed three times with 1 mL HBSS. Then, the Transwell plate was preincubated in HBSS at 37°C for 15 minutes. After the preincubation, 5 μM THC, 0.3 μM 11-OH-THC, or 2.5 μM THC-COOH with 50 μM LY in the presence or absence of 5 μM tariquidar for MDCKII-P-gp cells or 5 μM Ko143 for MDCKII-BCRP cells was added to the donor chamber (either the apical or the basolateral chamber) to final concentrations as shown above. The organic solvent concentration was kept at no more than 0.2% (v/v) for all assays. At 0 and 120 minutes of the assay, samples of 5 μL each were collected from the donor chamber, and samples of 100 μL each from the receiver chamber were collected at 30, 60, 90, and 120 minutes. The donor samples were diluted to a final volume of 100 μL with HBSS. After the last time point, cells were washed with ice-cold HBSS three times to terminate transporter activity. Cells were then lysed with 10% ACN for 1 hour at room temperature, and cell lysates were collected and vortexed, and 100 μL was used for analysis. Meanwhile, 2 μM quinidine (a P-gp probe substrate) or 3 μM prazosin (a BCRP probe substrate) was used as a positive control on a separate Transwell plate for MDCKII-P-gp or MDCKII-BCRP cells, respectively. For the positive control experiments, samples from the donor chamber were collected at 0 and 60 minutes, and samples from the receiver chamber were collected at 15, 30, 45, and 60 minutes. THC, 11-OH-THC, THC-COOH, quinidine, or prazosin in all samples were spiked with 100 μL of internal standards (250 nM d^3-THC for THC and THC-COOH, 250 nM d^3-11-OH-THC for 11-OH-THC, and 10 nM d^8-loperamide for quinidine and prazosin) and vortexed before centrifugation at 19,083*g* for 10 minutes at 4°C. Finally, 100 μL of supernatant was collected and subject to quantification using a validated liquid chromatography–tandem mass spectrometry (LC-MS/MS) assay as described below. For quinidine and prazosin samples, LY was determined as an indication of paracellular tight junction using a fluorescence microplate reader under 430 nm for excitation and 538 nm for emission. The apparent permeability for LY was no more than 2×10^{-6} cm/s in all Transwell transport assays estimated using the same equation below, and dQ/dt refers to change in absorption.

The apparent permeability (P_{app}) was calculated using the equation $P_{app} = (dQ/dt)/(c_0 * Area)$, with a unit of centimeters per second, when the steady-state assumption was met, where dQ/dt is the change in amount divided by incubation time, Area is the cell growth area on the Transwell insert, and c_0 is the initial concentration of a compound added to the donor chamber. If the steady-state assumption was not met, the initial concentration in the donor chamber declined substantially over time, and then P_{app} was calculated using the equation $P_{app} = Q_{receiver,\ last}/(AUC_{0\rightarrow last,\ donor} * Area)$, where $Q_{receiver,\ last}$ is the amount of a compound appeared in the receiver chamber at the last time point, and $AUC_{0\rightarrow last,\ donor}$ is the area under the concentration-time curve of the compound from time 0 to the last time point in the donor chamber. The efflux ratio (ER) was calculated as $P_{app,B\rightarrow A}/P_{app,A\rightarrow B}$, where $P_{app,\ A\rightarrow B}$ is the apparent permeability of a compound from the apical to the basolateral side, and $P_{app,\ B\rightarrow A}$ is the apparent

Downloaded from dmd.aspetjournals.org at ASPET Journals on October 14, 2022

permeability of the compound from the basolateral to the apical side. The mass balance of a compound in the Transwell system at the last time point was calculated as $(A_R + A_{IC} + A_D)/A_{D0}$, where A_R is the amount of the compound in the receiver at the last time point, A_{IC} is the intracellular amount of the compound at the last time point, A_D is the amount of the compound in the donor at the last time point, and A_{D0} is the amount of the compound in the donor at time 0. The contribution of the compound in the donor (A_D), receiver (A_R), and intracellular compartment (A_{IC}) to mass balance was calculated as a percentage of the total amount ($A_R + A_{IC} + A_D$).

Cellular Accumulation Assay. MDCKII cells overexpressing human P-gp or BCRP were seeded onto Collagen I–coated 24-well plates with a density of approximately 5×10^5 cells per well and cultured for 24 hours. On the day of the assay, each well was washed three times with 0.5 mL of HBSS and preincubated in HBSS in the presence or absence of an inhibitor (5 μM tariquidar for P-gp or 5 μM Ko143 for BCRP) at 37°C for 30 minutes. After the preincubation, 5 μM THC, 0.3 μM 11-OH-THC, or 2.5 μM THC-COOH was added to each well in the presence or absence of an inhibitor to final concentrations as shown above and incubated for 15, 30, 45, and 60 minutes. The organic solvent concentration was kept no more than 0.2% (v/v) for all assays. Meanwhile, 2 μM quinidine or 3 μM prazosin in the presence or absence of an inhibitor was used as a positive control on a separate plate for MDCKII-P-gp or MDCKII-BCRP cells, respectively. At each time point, cells were washed three times with 1 mL ice-cold HBSS to quench transporter activity. Cells were then lysed with 0.5 mL of 10% ACN for 1 hour at room temperature, and cell lysates were then collected. In total, 100 μl of cell lysates was spiked with 100 μL of respective internal standards as described in the Transwell transport assay and subject to quantification of THC, 11-OH-THC, THC-COOH, quinidine, or prazosin using a validated LC-MS/MS assay as described below. Protein concentrations of cell lysates were determined by the bicinchoninic acid assay protein assay kit with bovine serum albumin as standard. The cellular accumulation of a test compound was calculated by normalizing the amount of the compound to the amount of protein in each well and expressed as picomoles per microgram protein. Then, the AUC of cellular accumulation of the compounds was calculated using trapezoidal rule.

Vesicular Transport Assay. We used inside-out plasma membrane vesicles to determine whether THC, 11-OH-THC, and THC-COOH are inhibitors of P-gp and BCRP. A rapid filtration protocol modified from a previously reported method was used for vesicular transport assays of NMQ (a P-gp substrate) (Han et al., 2019) and LY (a BCRP substrate) (Deng et al., 2016). All test compounds, vesicles, and ATP/AMP were prepared in an incubation buffer (pH 7.0) containing 10 mM Tris-HCl, 10 mM $MgCl_2$, and 250 mM sucrose. Prior to initiation of P-gp–mediated transport reactions, 25 μL of 3 μM NMQ containing the solvent DMSO alone, tariquidar, or a cannabinoid was preincubated with 25 μL of 1 mg protein per milliliter vesicles at 37°C for 10 minutes. Reactions were then initiated by adding prewarmed 25 μL of 15 mM Mg-ATP or AMP and continued to incubate at 37°C for 5 minutes. The final concentrations of NMQ, THC, 11-OH-THC, THC-COOH, and ATP or AMP in the vesicular transport reactions were 1 μM, 1667 nM, 100 nM, 833.3 nM, and 5 mM, respectively. The reactions were stopped by adding 200 μL of ice-cold washing buffer (10 mM Tris-HCl, 100 mM NaCl, and 250 mM sucrose) and transferred to a prewet 96-well rapid filtration plate. Each well was washed five times with 200 μL of ice-cold washing buffer under vacuum. The NMQ trapped in the vesicles was eluted by adding 200 μL of ACN containing 100 nM quinidine as an internal standard under vacuum. The eluents were centrifuged under 19,083*g* for 10 minutes at 4°C, and 50 μL of supernatant was subject to quantification using LC-MS/MS as described below. In the case of BCRP-mediated vesicular transport, a final concentration of 50 μM LY and 15 μg of vesicle protein per reaction were used and incubated for 10 minutes, and reactions were initiated and incubated as described above. The elution was performed using 100 μL of 0.1 M NaOH, and the eluent was neutralized with 100 μL of 0.1 M HCl. LY in eluents was quantified by measuring fluorescence with excitation at 430 nm and emission at 538 nm. In all vesicular transport assays, the organic solvent concentration was kept no more than 0.2% (v/v). ATP-dependent uptake of NMQ or LY into membrane vesicles was calculated by subtracting the uptake in the presence of AMP from that in the presence of ATP and normalized as a percentage of the positive control. ATP-dependent uptake of NMQ or LY with DMSO alone was used as a positive control and set to 100%.

LC-MS/MS Analysis. All samples including cell lysates were analyzed using an AB Sciex Triple Quad 6500 (SCIEX, Framingham, MA) coupled with the Acquity ultraperformance liquid chromatography system (Waters, Milford, MA). Acquity ultraperformance liquid chromatography BEH C_{18} column (1.7 μM, 2.1 × 50 mm) attached to the C_{18} × 2-mm guard column was used for chromatography analysis. The organic and aqueous phases used were water and ACN containing 0.1% formic acid, respectively (as solvents A and B, respectively). The mass spectrometer was operated in the positive electrospray ionization mode. The interday and intraday variance for quality control samples were no more than 15%, and standard curves were established with $1/y^2$ weighting. Liquid chromatography flow gradient and multiple reaction monitoring parameters used for quantification of cannabinoids were the same as previously described (Patilea-Vrana et al., 2019). For quantification of quinidine and prazosin, the flow rate was 0.3 mL/min, and the gradient conditions were as follows: starting 95% A in the first 2 minutes, changed to 5% A for the next 55 seconds, and then switched to 95% A again and maintained until 4 minutes. The temperature of column was maintained at 45°C, and the autosampler was maintained at 4°C. The injection volume was 10 μL. Analytes were quantified by the following transitions: quinidine 31.000 > 32.000 m/z; prazosin, 45.000 > 40.000 m/z; d^8-loperamide, 25.000 > 20.000 m/z. For the quantification of NMQ, the flow rate was 0.5 mL/min, and the gradient conditions were as follows: starting 90% A in the first 1.2 minutes, changed to 5% A and maintained until 4 minutes, and switched back to 90% A for the following 30 seconds. The temperature of column was maintained at 45°C, and the autosampler was maintained at 6°C. The injection volume was 10 μL. Analytes were quantified by the 339.30 > 339.30 with 11 V collision energy. Integration of the chromatographic peaks was performed using Analyst v1.6 (Framingham, MA). The relative concentrations of a test compound in a sample were expressed as the peak area ratios of the compound to internal standard for Transwell assays, and the ratios were converted to molar concentration according to the standard curve for cellular accumulation and vesicular transport assays.

Statistical Analysis. At least three independent experiments were performed for the Transwell transport (except for THC) and cellular accumulation assays with triplicate in each experiment, or for the vesicular transport assay with duplicate in each experiment. Data were reported as means ± S.D. of at least three independent experiments using mean values in each experiment. Differences in transport activity between with and without an inhibitor or between A → B and B → A transport were analyzed by the paired Student's *t* test, two-way ANOVA followed by the Šidák's *post hoc* test, or paired two-way ANOVA followed by the Tukey's *post hoc* test for Transwell transport and cellular accumulation assays. For the vesicular transport assay, all comparisons were analyzed by paired one-way ANOVA followed by the Dunnett's *post hoc* test. Differences with P values of < 0.05 were considered statistically significant. All the analysis was performed using GraphPad Prism 8 (La Jolla, CA).

Results

Bidirectional Transwell Transport of Cannabinoids in MDCKII-P-gp Cells. To investigate whether THC, 11-OH-THC, and THC-COOH are substrates of human P-gp, we first performed the bidirectional Transwell transport assay on the MDCKII cell monolayers overexpressing human P-gp, with 2 μM quinidine as a probe substrate and 5 μM tariquidar as the P-gp inhibitor. The ER of quinidine, although variable, was much greater than 2 in the absence of tariquidar and decreased to ∼1 in the presence of tariquidar (Table 1), confirming good P-gp activity in MDCKII cells. For 11-OH-THC and THC-COOH, the ERs were around 1 in the presence and absence of tariquidar (Table 1), suggesting that these cannabinoids were not transported by P-gp. Because THC was not quantifiable in the receiver chamber, the ER of THC could not be determined. Therefore, we analyzed the mass balance of THC. We noted that, ∼80% of THC was trapped intracellularly when THC was tested in the A → B direction regardless of whether tariquidar was present (Table 2). When THC was tested in the B → A direction, 100% and ∼85% of THC were trapped in the cells in the absence and presence of tariquidar, respectively (Table 2). And generally, less than 5% of THC appeared in the receiver chamber (Table 2). We also observed intracellular trapping of 11-OH-THC and THC-COOH, but to a much lesser extent, and the metabolites were

Downloaded from dmd.aspetjournals.org at ASPET Journals on October 14, 2022

TABLE 1

Efflux ratios of 11-OH-THC and THC-COOH in MDCKII-P-gp cells in Transwell transport assays

Data shown are means ± S.D. of three independent experiments with triplicate in each experiment. ER was calculated as the ratio of individual $P_{app,\ B\rightarrow A}$ to its corresponding $P_{app,\ B\rightarrow A}$. Differences in ERs between DMSO and tariquidar in each treatment group were analyzed by the paired Student's t test. ER of THC is not shown here because THC could not be detected in the receiver compartment (see Results for details).

Group	Compound	Treatment	ER	Level of Significance
11-OH-THC	0.3 μM 11-OH-THC	DMSO	0.98 ± 0.46	NS
(n = 3)		5 μM tariquidar	0.90 ± 0.42	
	2 μM Quinidine	DMSO	10.69 ± 7.45	P = 0.0473
		5 μM tariquidar	1.01 ± 0.35	
THC-COOH	2.5 μM THC-COOH	DMSO	1.04 ± 0.40	NS
(n = 3)		5 μM tariquidar	0.74 ± 0.05	
	2 μM Quinidine	DMSO	6.01 ± 1.13	P = 0.0050
		5 μM tariquidar	1.26 ± 0.12	

quantifiable in the receiver chamber (Table 2). These results suggested that, because of high intracellular trapping of THC, the Transwell system is not suitable to determine ER for THC. Thus, cellular accumulation assay was used as an alternative to investigate whether THC is a P-gp substrate and verify the Transwell transport data for 11-OH-THC and THC-COOH (see below).

Cellular Accumulation of Cannabinoids in MDCKII-P-gp Cells. To verify the observations in the Transwell transport assays that the cannabinoids were not transported by P-gp and to resolve the issues mentioned above in the Transwell transport assay for THC, we performed unidirectional cellular accumulation assay using MDCKII-P-gp cells. The cellular accumulation of quinidine, THC, 11-OH-THC, and THC-COOH in a representative experiment is shown in Fig. 1. The AUCs of cellular accumulation were then calculated from at least three independent experiments and compared between the presence and absence of 5 μM tariquidar (Table 3). Although the activity of P-gp varied among different passages of cells (2.47-fold change in the ratio of AUC with tariquidar to the AUC without tariquidar for quinidine from 1.50 to 3.71), the AUC of cellular accumulation for quinidine in the presence of tariquidar was significantly greater than that in the absence of tariquidar, and the average AUC ratios in the presence and absence of tariquidar for quinidine were greater than 2 (Table 3), confirming P-gp activity in MDCKII-P-gp cells. In contrast, the cellular accumulation of THC, 11-OH-THC, and THC-COOH were not significantly different between the presence and absence of tariquidar as shown in the representative experiment (Fig. 1). Likewise, the AUCs of cellular accumulation for THC, 11-OH-THC, and THC-COOH in the presence of tariquidar were not significantly different from those in the absence of tariquidar, with the AUC ratios of around 1 for all the cannabinoids (Table 3). These results further supported that THC, 11-OH-THC, and THC-COOH are not P-gp substrates.

Bidirectional Transwell Transport of Cannabinoids in MDCKII-BCRP Cells. Next, we performed the Transwell transport assay for the cannabinoids using MDCKII-BCRP cells, with prazosin (3 μM) as a probe substrate and Ko143 (5 μM) as the BCRP inhibitor. The ERs of prazosin in the absence of Ko143 were much greater than 2 and were decreased to approximately 1 in the presence of Ko143 (Table 4), confirming BCRP activity in the MDCKII cells. Similar to what we observed in MDCKII-P-gp cells, 60%–100% of THC was trapped in MDCKII-BCRP cells, and THC in the receiver chamber was not quantifiable, whereas 11-OH-THC and THC-COOH were trapped in cells to a lesser extent (Table 2). For 11-OH-THC, its ERs in the

TABLE 2

Mass balance of cannabinoids in bidirectional Transwell transport assays

Data shown for THC are means of duplicate experiments, each conducted in triplicate, and for 11-OH-THC and THC-COOH are means ± S.D. of at least three independent experiments, each conducted in triplicate, in the absence (−) and presence (+) of an inhibitor. Mass balance data were expressed as percentage of the total mass quantified for the three compartments.

MDCKII-P-gp		A→B		B→A	
Mass balance (%)	5 μM tariquidar	−	+	−	+
THC	Receiver	0	3.86	0	0.32
(n = 2)	Donor	19.82	18.86	0	14.11
	Intracellular	80.18	77.28	100	85.57
11-OH-THC	Receiver	4.89 ± 1.23	4.21 ± 0.70	2.71 ± 0.39	2.68 ± 1.06
(n = 3)	Donor	24.06 ± 11.99	23.57 ± 11.40	73.25 ± 4.18	73.04 ± 9.53
	Intracellular	71.04 ± 10.87	72.22 ± 11.06	24.04 ± 4.04	24.28 ± 8.52
THC-COOH	Receiver	16.46 ± 3.69	21.35 ± 7.75	10.66 ± 2.42	10.78 ± 2.90
(n = 3)	Donor	44.37 ± 15.30	38.43 ± 13.41	76.35 ± 6.21	75.76 ± 5.32
	Intracellular	39.18 ± 17.49	40.22 ± 21.12	12.99 ± 8.59	13.45 ± 8.20
MDCKII-BCRP		A→B		B→A	
Mass balance (%)	5 μM Ko143	−	+	−	+
THC	Receiver	0	0	0	0.22
(n = 2)	Donor	11.17	15.07	40.10	0
	Intracellular	88.83	84.93	59.90	99.78
11-OH-THC	Receiver	6.07 ± 1.49	6.85 ± 2.52	3.06 ± 1.65	3.55 ± 1.29
(n = 4)	Donor	24.04 ± 5.48	24.93 ± 5.01	72.89 ± 7.61	70.83 ± 6.67
	Intracellular	69.89 ± 4.17	68.22 ± 2.92	24.05 ± 6.04	25.63 ± 5.42
THC-COOH	Receiver	23.04 ± 7.07	25.62 ± 4.38	15.78 ± 3.02	12.59 ± 1.19
(n = 3)	Donor	47.98 ± 16.68	43.51 ± 7.57	75.23 ± 8.07	76.09 ± 1.19
	Intracellular	28.98 ± 10.15	30.86 ± 6.04	8.99 ± 5.09	11.32 ± 2.03

Downloaded from dmd.aspetjournals.org at ASPET Journals on October 14, 2022

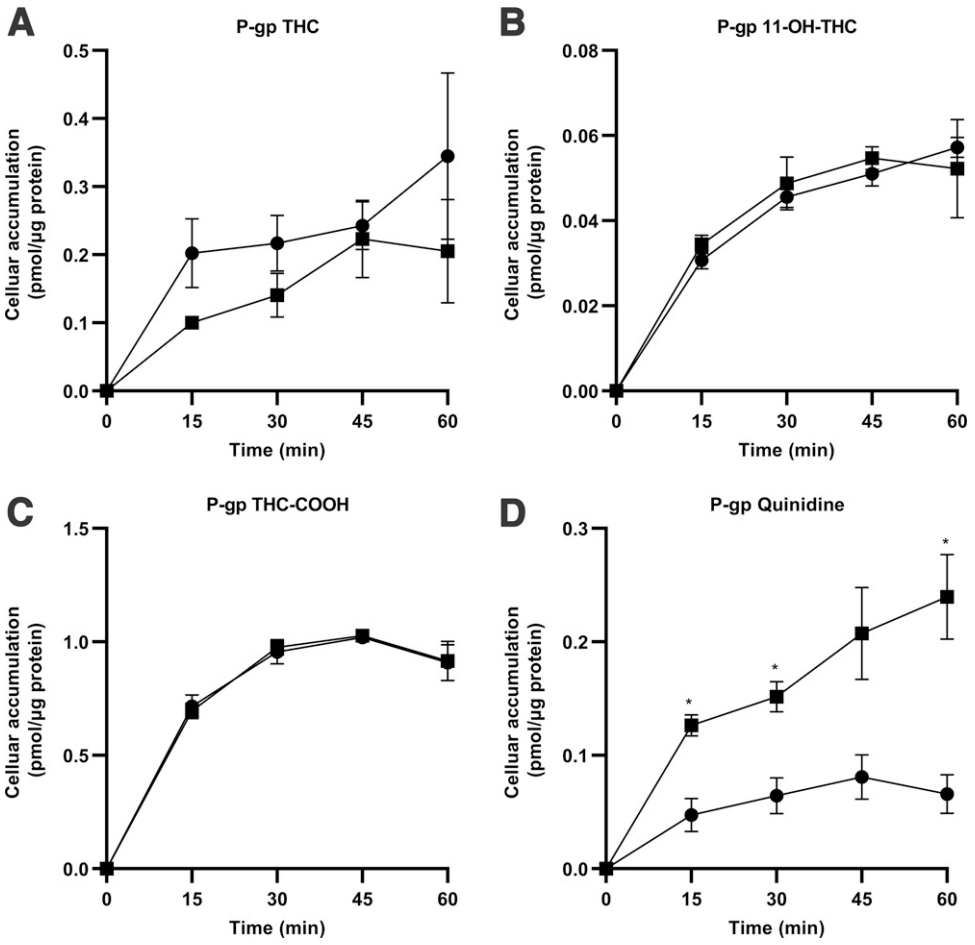

Fig. 1. Cellular accumulation of THC, 11-OH-THC, or THC-COOH in MDCKII-P-gp cells in a representative experiment. Cellular accumulation of 5 μM THC (A), 0.3 μM 11-OH-THC (B), 2.5 μM THC-COOH (C), and 2 μM quinidine (D) in MDCKII-P-gp cells in the absence (solid circles) or presence (solid squares) of 5 μM tariquidar in a representative experiment. Data shown are means ± S.D. of triplicates. Differences in cellular accumulation in the absence and presence of tariquidar were analyzed using two-way ANOVA followed by the Šidák's *post hoc* test. $*P < 0.05$.

presence and absence of Ko143 were around 1 (Table 4), indicating that 11-OH-THC was not transported by BCRP. Interestingly, the ERs of THC-COOH in the absence of Ko143 were ∼1.6 and were significantly decreased to ∼1.0 in the presence of Ko143 (Table 4), suggesting that THC-COOH is a weak substrate of BCRP. Transwell transport of THC-COOH and the BCRP probe substrate prazosin is shown in Fig. 2.

Cellular Accumulation of Cannabinoids in MDCKII-BCRP Cells. We also performed the monodirectional cellular accumulation assay for these cannabinoids using MDCKII-BCRP cells, and the cellular accumulation data for prazosin, THC, 11-OH-THC, and THC-COOH from a representative experiment are shown in Fig. 3. Although the activity of BCRP varied with different cell passages (6.13-fold change in the ratio of AUC with Ko143 to the AUC without Ko143 for prazosin from 7.86 to 48.2), the AUCs of cellular accumulation for prazosin in the presence of Ko143 were significantly greater than those in the absence of Ko143, with the average AUC ratios in the presence over the absence of Ko143 of >20 (Table 5), confirming BCRP activity in MDCKII-BCRP cells. The AUCs for THC or 11-OH-THC in the presence and absence of Ko143 were not significantly different, with the AUC ratio of around 1; however, the AUC for THC-COOH in the presence of Ko143 was significantly greater than that in the absence of Ko143, with the AUC ratio of ∼1.6 (Table 5). These results confirmed that THC-COOH is a weak substrate of BCRP, but THC and 11-OH-THC are not.

Inhibition of P-gp– or BCRP-Mediated Vesicular Transport by Cannabinoids. Finally, we investigated whether these cannabinoids are inhibitors of human P-gp and BCRP at pharmacologically relevant concentrations. We performed vesicular transport assay using NMQ and LY as the probe substrates for P-gp and BCRP, respectively. We used THC at 1667 nM, 11-OH-THC at 100 nM, and THC-COOH at 833.3

TABLE 3

Cellular accumulation of cannabinoids in MDCKII-P-gp cells

Shown are the AUC ratios of cellular accumulation for 5 μM THC, 0.3 μM 11-OH-THC, and 2.5 μM THC-COOH in MDCKII-P-gp cells in the absence or presence of 5 μM tariquidar. Quinidine (2 μM) was used as a P-gp positive control probe substrate. The AUCs were calculated using the trapezoidal rule with 0, 15, 30, 45, and 60 min as the time points. Data shown are means ± S.D. from at least three independent experiments (n = 4 for THC; n = 5 for 11-OH-THC; and n = 3 for THC-COOH), each conducted in triplicate. Differences in AUC ratio between the absence and presence of tariquidar were analyzed using the paired Student's t test.

Group	Treatment	AUC Ratio	Level of Significance
THC	5 μM THC	1.16 ± 0.59	NS
(n = 4)	2 μM quinidine	2.30 ± 0.99	P = 0.03
11-OH-THC	0.3 μM 11-OH-THC	1.09 ± 0.08	NS
(n = 5)	2 μM quinidine	2.32 ± 0.54	P = 0.002
THC-COOH	2.5 μM THC-COOH	0.96 ± 0.06	NS
(n = 3)	2 μM quinidine	2.50 ± 0.40	P = 0.0113

Downloaded from dmd.aspetjournals.org at ASPET Journals on October 14, 2022

TABLE 4

Efflux ratios of 11-OH-THC or THC-COOH in MDCKII-BCRP cells in Transwell assays

Data shown are means ± S.D. of at least three independent experiments with triplicate in each experiment (n = 4 for the 11-OH-THC group; n = 3 for the THC-COOH group). ER was calculated as the ratio of individual $P_{app,\ B\rightarrow A}$ to its corresponding $P_{app,\ A\rightarrow B}$. Differences in ERs between DMSO and Ko143 in each treatment group were analyzed by the paired Student's t test. ER of THC is not shown here because THC could not be detected in the receive compartment (see Results for details).

Group	Compound	Treatment	ER	Level of Significance
11-OH-THC (n = 4)	0.3 μM 11-OH-THC	DMSO	0.78 ± 0.09	NS
		5 μM Ko143	0.96 ± 0.30	
	3 μM Prazosin	DMSO	5.48 ± 0.61	P = 0.0004
		5 μM Ko143	0.97 ± 0.13	
THC-COOH (n = 3)	2.5 μM THC-COOH	DMSO	1.61 ± 0.12	P = 0.0101
		5 μM Ko143	1.01 ± 0.13	
	3 μM Prazosin	DMSO	7.75 ± 4.19	P = 0.0248
		5 μM Ko143	0.77 ± 0.08	

nM to represent their respective pharmacologically relevant total plasma concentrations observed in humans (Cox et al., 2019). As expected, tariquidar at 166.7 nM and 500 nM significantly inhibited P-gp–mediated ATP-dependent vesicular uptake of NMQ (Fig. 4A). Likewise, Ko143 at 33.33 nM and 100 nM significantly inhibited BCRP-mediated ATP-dependent vesicular uptake of LY (Fig. 4B). These results indicated that P-gp and BCRP in the plasma membrane vesicles were functional. We did not observe significant inhibition of ATP-dependent vesicular uptake of NMQ by any of the cannabinoids at pharmacologically relevant concentration (Fig. 4A). Likewise, we did not observe significant inhibition of ATP-dependent vesicular uptake of LY by THC or 11-OH-THC (Fig. 4B). However, THC-COOH at 833.3 nM inhibited ATP-dependent vesicular uptake of LY by 48.7% (Fig. 4B), suggesting that THC-COOH is a BCRP inhibitor at a pharmacologically relevant concentration. Collectively, these results indicated that THC-COOH is an inhibitor of BCRP, but not of P-gp, and neither THC nor 11-OH-THC is an inhibitor of both P-gp and BCRP at pharmacologically relevant total plasma concentrations.

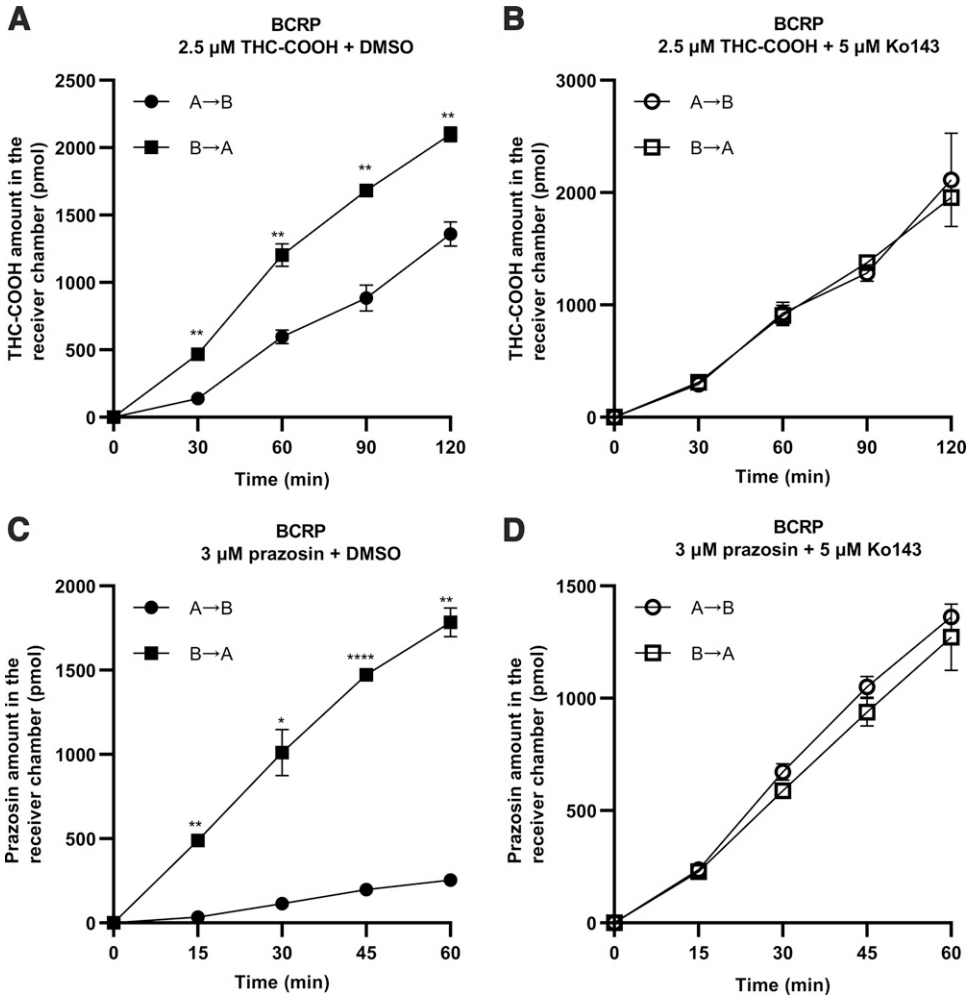

Fig. 2. Transwell transport of THC-COOH by BCRP in MDCKII-BCRP cells. Shown are the Transwell transport data of 2.5 μM THC-COOH (A and B) and 3 μM prazosin (C and D) in MDCKII-BCRP cells in the absence (solid circles for A→B, and solid squares for B→A) or presence (open circles for A→B, and open squares for B→A) of 5 μM Ko143. Data shown are means ± S.D. of triplicates. Differences in transport between the A→B and B→A directions at each time point were analyzed using paired two-way ANOVA followed by the Tukey's *post hoc* test. *$P < 0.05$; **$P < 0.01$; ***$P < 0.001$; ****$P < 0.0001$.

Downloaded from dmd.aspetjournals.org at ASPET Journals on October 14, 2022

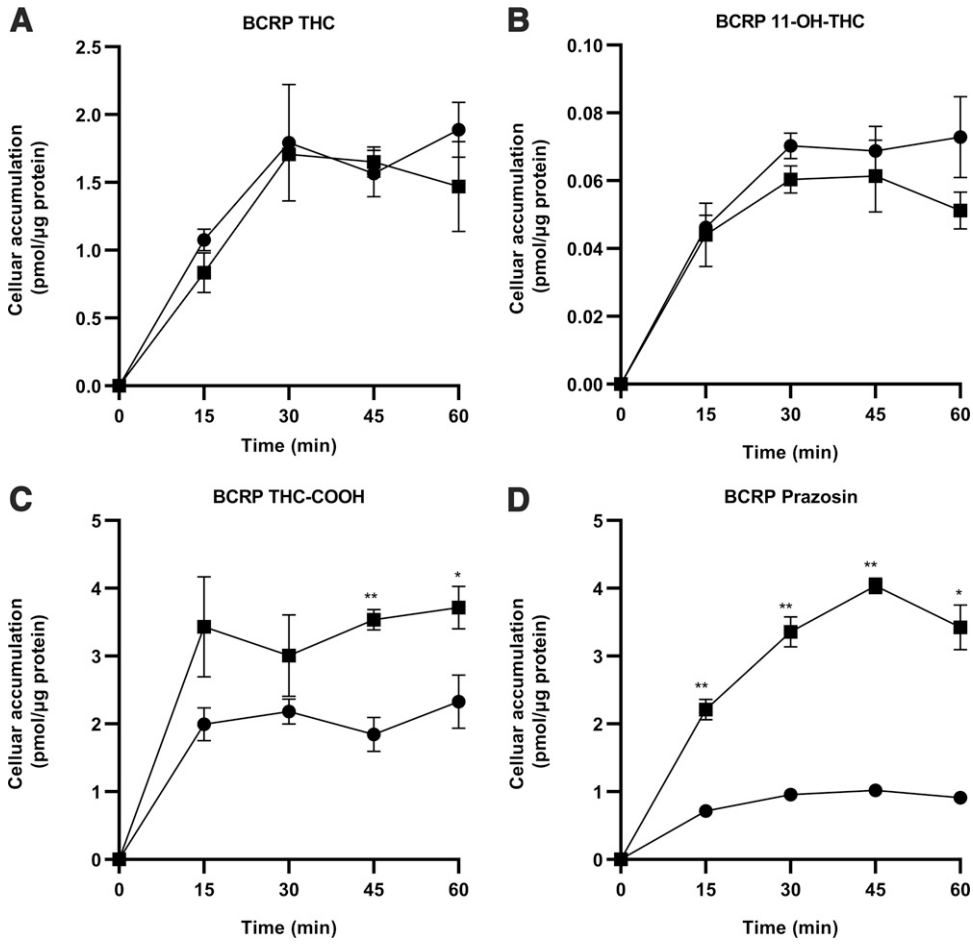

Fig. 3. Cellular accumulation of THC, 11-OH-THC, and THC-COOH in MDCKII-BCRP cells in a representative experiment. Shown are cellular accumulation data for 5 μM THC (A), 0.3 μM 11-OH-THC (B), 2.5 μM THC-COOH(C), and 3 μM prazosin (D) in MDCKII-BCRP cells in the absence (solid circles) or presence (solid squares) of 5 μM Ko143 in a representative experiment with triplicates. Data shown are means ± S.D. from triplicates in the experiment. Differences in cellular accumulation between the absence and presence of Ko143 were analyzed using two-way ANOVA followed by the Šidák's *post hoc* test. $*P < 0.05$; $**P < 0.01$.

Discussion

In this study, we systematically performed Transwell, cellular accumulation, and vesicular transport studies for THC, 11-OH-THC, and THC-COOH using MDCKII cells or plasma membrane vesicles overexpressing human P-gp or BCRP to investigate whether these cannabinoids are substrates or inhibitors at pharmacologically relevant concentrations.

Three aforementioned assays were used, as each has advantages and disadvantages in detecting whether a compound of interest is a substrate or an inhibitor of an efflux transporter. The Transwell assay is considered to be optimal and superior to the cellular accumulation assay in detecting efflux transport of lipophilic compounds such as the cannabinoids. This is because in the cellular accumulation assay, the transport signal may be overwhelmed by passive diffusion or partitioning of the compound into the cells or cell membrane. In contrast, in the Transwell assay, although a lipophilic compound will also extensively partition into the cells/cell membrane, its appearance in the receiver compartment (if detectable) can detect passive transfer or efflux transport of the compound with high sensitivity. Therefore, to determine whether the cannabinoids are transported by P-gp or BCRP, our first choice was to use the Transwell assay with cells overexpressing P-gp or BCRP. However, because of extensive intracellular binding and accumulation, we were unable to detect the appearance of THC in the receiver compartment, making this assay unusable. Since THC seems to extensively partition into the cells and presumably into the cell membrane, we speculated that the cellular accumulation assay may be able to detect P-gp–mediated efflux of THC since this transporter acts as a vacuum cleaner to remove substrates from the

TABLE 5

Cellular accumulation of cannabinoids in MDCKII-BCRP cells

Shown are the AUC ratios of cellular accumulation for 5 μM THC, 0.3 μM 11-OH-THC, and 2.5 μM THC-COOH in MDCKII-BCRP cells in the absence or presence of 5 μM Ko143. Prazosin (3 μM) was used as a BCRP positive probe substrate. The AUCs were calculated using the trapezoidal rule with 0, 15, 30, 45, and 60 min as the time points. Data shown are means ± S.D. of quadruplicate with triplicate in each experiment. Differences in AUC ratio between the absence and presence of Ko143 were analyzed using the paired Student's t test.

Group	Treatment	AUC Ratio	Level of Significance
THC	5 μM THC	0.83 ± 0.06	NS
(n = 4)	3 μM prazosin	20.04 ± 11.77	P = 0.0034
11-OH-THC	0.3 μM 11-OH-THC	1.25 ± 0.32	NS
(n = 4)	3 μM prazosin	29.01 ± 16.61	P = 0.0039
THC-COOH	2.5 μM THC-COOH	1.61 ± 0.09	P = 0.0005
(n = 4)	3 μM prazosin	28.42 ± 7.07	P = 0.0002

Downloaded from dmd.aspetjournals.org at ASPET Journals on October 14, 2022

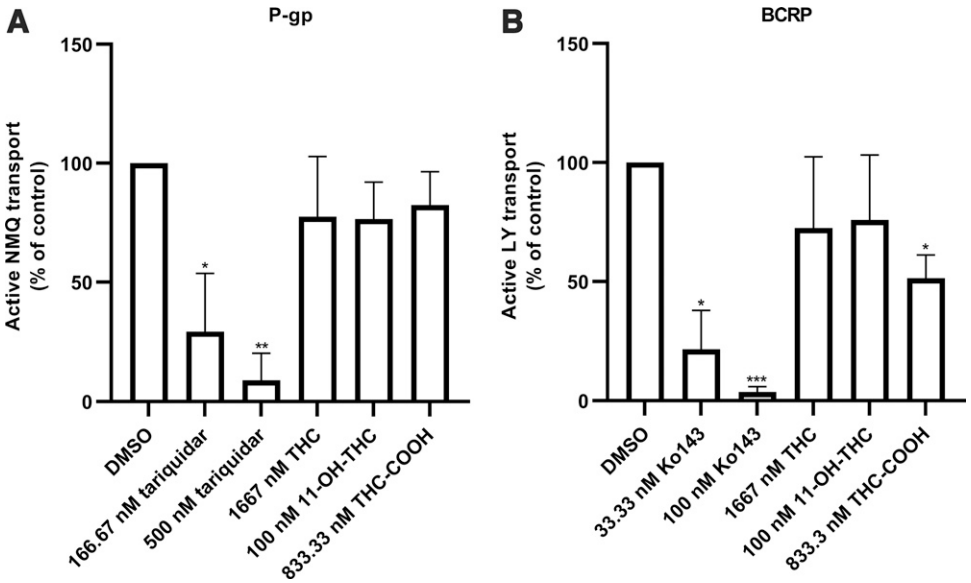

Fig. 4. Inhibition of P-gp– or BCRP-mediated vesicular transport by THC, 11-OH-THC, or THC-COOH. Inhibition of P-gp– or BCRP-mediated vesicular transport by THC, 11-OH-THC, or THC-COOH at pharmacologically relevant concentrations was assessed using inside-out plasma membrane vesicles overexpressing human P-gp (A) or BCRP (B). Data shown are means ± S.D. of triplicates with duplicate in each experiment. The final concentrations of NMQ (P-gp probe substrate) and LY (BCRP probe substrate) were 1 μM and 50 μM, respectively. Statistically significant differences between all treatment groups were evaluated using paired one-way ANOVA followed by the Dunnett's *post hoc* test for multiple comparisons. * $P < 0.05$; ** $P < 0.01$; *** $P < 0.001$.

lipid bilayer of cell membrane. Finally, the vesicular transport assay, using hydrophilic substrates and the cannabinoids as inhibitors, is a simple and rapid method to determine whether a compound is an inhibitor of an efflux transporter.

Cannabinoids are highly lipophilic molecules with low aqueous solubility (Garrett and Hunt, 1974). THC solubility in pure water is estimated to be 8.9 μM and will decrease when ionic strength of solution increases (Garrett and Hunt, 1974). The presence of organic solvent significantly increases THC solubility (Garrett and Hunt, 1974). However, excess organic solvent can alter protein expression profiles of cells and/or disrupt cell membrane (Busby et al., 1999); therefore, we kept organic solvent concentration at 0.2% (v/v) to minimize the impact of organic solvent on cells and membrane vesicles. This low organic solvent concentration and salts in transport buffers limit the solubility of cannabinoids in the final transport buffers. These solubility issues of cannabinoids have been well recognized in previous cannabinoid metabolism studies (Patilea-Vrana and Unadkat, 2019; Bansal et al., 2020). Although higher THC solubility may be achieved in fasted-state and fed-state simulated intestinal fluids to be approximately 28 μM and 36 μM, respectively (Bansal et al., 2020), bile acids (Deng et al., 2016) and surfactants in the intestinal fluids may interfere with both cell-based and vesicular transport assays.

Therefore, largely because of solubility issues, we used 5 μM THC, 0.3 μM 11-OH-THC, and 2.5 μM THC-COOH in the Transwell and cellular accumulation assays, which are the highest possible concentrations we could achieve as a result of low organic solvent concentration in transport buffers and the cannabinoid concentrations in stock solutions available to us. We chose these concentrations also because they are comparable to the total human plasma concentrations of these cannabinoids (Cox et al., 2019). Cox et al. (2019) summarized that the highest total reported plasma concentrations of THC, 11-OH-THC, and THC-COOH after THC administration are 1392 nM (intravenous), 69.2 nM (oral), and 519 nM (oral), respectively. Given high plasma protein binding of THC (98.9%), 11-OH-THC (98.8%) (Patilea-Vrana and Unadkat, 2019), and THC-COOH (assumed to be 98.8%) (Bansal et al., 2020), the cannabinoid concentrations used in this study are much greater than the unbound human plasma concentrations of these cannabinoids. The Transwell and cellular accumulation assays revealed that THC and 11-OH-THC are not substrates of P-gp or BCRP, and THC-COOH is not a substrate of P-gp. The exception was that THC-COOH was weakly transported by BCRP, with an ER of less than 2. Based on Food and Drug Administration guidelines (US Food and Drug Administration, 2020), THC-COOH is classified as a poor BCRP substrate.

In the Transwell studies, we showed that 80%–100% of THC was trapped intracellularly. Given its extremely high plasma protein binding (Garrett and Hunt, 1974), THC could tightly bind to intracellular proteins, such as fatty acid–binding proteins, which are known to be intracellular carriers for THC in HeLa cells (Elmes et al., 2015). These findings provide novel insights into our understanding and interpretation of *in vivo* animal and human data. For example, because of its high lipophilic nature, THC could readily get into the placental syncytiotrophoblasts from the maternal circulation by passive diffusion. Once in the cells, THC may remain in the placenta via tight intracellular protein binding. Thus, the lower fetal exposure to THC versus its maternal exposure observed in the pregnant macaque study could be due to sequestration of THC in the placental tissue (Bailey et al., 1987). Hence, the observation of fetal/maternal plasma AUC ratio of <1 may not be due to P-gp– and/or BCRP-mediated efflux of THC by the placenta. Human placenta perfusion studies are currently underway in our laboratory to confirm that THC and 11-OH-THC are not substrates of P-gp and/or BCRP. This confirmation is important for understanding and prediction of fetal and placental exposure to cannabinoids as well as their consequent fetal and placental toxicity. Interestingly, studies in *P-gp/Bcrp* knock-out mice show that THC is a weak substrate of intestinal P-gp (after oral THC administration) (Bonhomme-Faivre et al., 2008), although the data on brain distribution of THC are less convincing since they show an effect on brain concentrations of THC at only some sampling times, rather than an effect on brain/plasma AUC ratios (Spiro et al., 2012). Therefore, animal data regarding whether THC is a substrate of mouse P-gp and/or Bcrp remain inconclusive. We are currently conducting animal studies to further investigate whether P-gp and/or Bcrp plays a role in the fetal distribution of these cannabinoids.

Previous studies reported that THC and THC-COOH stimulate the ATPase activity of P-gp (Zhu et al., 2006), suggesting that these cannabinoids do interact with P-gp. P-gp substrates can either stimulate or inhibit its ATPase activity (Loo et al., 2003). Moreover, a substance that can stimulate ATPase activity of P-gp may not be a substrate of the transporter (Mi and Lou, 2007). Therefore, stimulation of ATPase activity does not necessarily mean THC and THC-COOH are P-gp substrates. Our data suggest that the interaction of P-gp with cannabinoids

Downloaded from dmd.aspetjournals.org at ASPET Journals on October 14, 2022

(if any) did not result in P-gp transport of THC or THC-COOH. Another possibility is that these cannabinoids are inhibitors of P-gp or BCRP. Tournier et al. (2010) reported that THC inhibits P-gp at 50 μM, and the inhibitory potency of 50 μM THC is ∼10-fold less than 5 μM valspodar. Tournier et al. (2010) also mentioned that THC at 50 μM weakly inhibits BCRP. Holland et al. (2007) also reported that THC inhibits BCRP. However, organic solvent concentrations (e.g., 2% ethanol) used to dissolve 10 or 50 μM THC in their assays were excessive and may be a complicating factor. THC concentrations used in these studies are not pharmacologically relevant and are greater than the water solubility of THC. The actual THC concentrations in their buffer solutions may be lower than the reported nominal concentrations.

To confirm whether the cannabinoids are inhibitors of human P-gp and BCRP at pharmacologically relevant concentrations, we performed the vesicular transport assay to determine their inhibitory potency for P-gp or BCRP. The concentrations of THC, 11-OH-THC, and THC-COOH used in the vesicular inhibition studies were 1667 nM, 100 nM, and 833.3 nM, respectively, which were higher than their highest total plasma concentrations reported to date (Cox et al., 2019). We found that THC-COOH at 833.3 nM can moderately inhibit BCRP-mediated transport of LY, indicating that THC-COOH is a weak or moderate BCRP inhibitor, consistent with our finding that THC-COOH is a weak substrate of BCRP. In contrast, THC-COOH does not inhibit P-gp, and neither THC nor 11-OH-THC is an inhibitor of P-gp or BCRP. Because of the limited cannabinoid solubility, we were not able to determine the IC_{50} value of the inhibition of P-gp or BCRP by the cannabinoids.

In summary, we have demonstrated that, at pharmacologically relevant concentrations, THC-COOH is a weak substrate and inhibitor of BCRP, but not of P-gp, and that THC and 11-OH-THC are neither substrates nor inhibitors of P-gp and BCRP. These results suggest that P-gp or BCRP will not modulate the brain and fetal distribution or intestinal absorption of these cannabinoids in humans. In addition, significant in vivo drug interactions between these cannabinoids and P-gp or BCRP inhibitors and inducers are unlikely. Future studies are needed to determine whether cannabinoids are substrates and inhibitors of other drug transporters.

Acknowledgments

The authors thank Dr. Per Artursson (Uppsala University, Sweden) for generously providing the CKII-hMDR1-cMDR1-KO cell line; Drs. Sumit Bansal, J. Scott Edgar, and Dale Whittington for technical assistance in using LC-MS/MS; and Drs. Abhinav Nath and Joanne Wang for allowing us to use their fluorescence microplate readers.

Authorship Contributions

Participated in research design: Chen, Unadkat, Mao.

Conducted experiments: Chen.

Performed data analysis: Chen.

Wrote or contributed to the writing of the manuscript: Chen, Unadkat, Mao.

References

Allikmets R, Schriml LM, Hutchinson A, Romano-Spica V, and Dean M (1998) A human placenta-specific ATP-binding cassette gene (ABCP) on chromosome 4q22 that is involved in multidrug resistance. *Cancer Res* **58**:5337–5339.

Aronica E, Gorter JA, Redeker S, van Vliet EA, Ramkema M, Scheffer GL, Scheper RJ, van der Valk P, Leenstra S, Baayen JC, et al. (2005) Localization of breast cancer resistance protein (BCRP) in microvessel endothelium of human control and epileptic brain. *Epilepsia* **46**:849–857.

Bailey JR, Cunny HC, Paule MG, and Slikker Jr W (1987) Fetal disposition of delta 9-tetrahydrocannabinol (THC) during late pregnancy in the rhesus monkey. *Toxicol Appl Pharmacol* **90**:315–321.

Bansal S, Maharao N, Paine MF, and Unadkat JD (2020) Predicting the potential for cannabinoids to precipitate pharmacokinetic drug interactions via reversible inhibition or inactivation of major cytochromes P450. *Drug Metab Dispos* **48**:1008–1017.

Bonhomme-Faivre L, Benyamina A, Reynaud M, Farinotti R, and Abbara C (2008) Disposition of Δ tetrahydrocannabinol in CF1 mice deficient in mdr1a P-glycoprotein. *Addict Biol* **13**:295–300.

Booth JK and Bohlmann J (2019) Terpenes in Cannabis sativa - From plant genome to humans. *Plant Sci* **284**:67–72.

Busby Jr WF, Ackermann JM, and Crespi CL (1999) Effect of methanol, ethanol, dimethyl sulfoxide, and acetonitrile on in vitro activities of cDNA-expressed human cytochromes P-450. *Drug Metab Dispos* **27**:246–249.

Carliner H, Brown QL, Sarvet AL, and Hasin DS (2017) Cannabis use, attitudes, and legal status in the U.S.: A review. *Prev Med* **104**:13–23.

Cox EJ, Maharao N, Patilea-Vrana G, Unadkat JD, Rettie AE, McCune JS, and Paine MF (2019) A marijuana-drug interaction primer: Precipitants, pharmacology, and pharmacokinetics. *Pharmacol Ther* **201**:25–38.

Deng F, Sjöstedt N, and Kidron H (2016) The effect of albumin on MRP2 and BCRP in the vesicular transport assay. *PLoS One* **11**:e0163886.

Doyle LA, Yang W, Abruzzo LV, Krogmann T, Gao Y, Rishi AK, and Ross DD (1998) A multidrug resistance transporter from human MCF-7 breast cancer cells. *Proc Natl Acad Sci USA* **95**:15665–15670.

Elmes MW, Kaczocha M, Berger WT, Leung K, Ralph BP, Wang L, Sweeney JM, Miyauchi JT, Tsirka SE, Ojima I, et al. (2015) Fatty acid-binding proteins (FABPs) are intracellular carriers for Δ9-tetrahydrocannabinol (THC) and cannabidiol (CBD). *J Biol Chem* **290**:8711–8721.

Fetsch PA, Abati A, Litman T, Morisaki K, Honjo Y, Mittal K, and Bates SE (2006) Localization of the ABCG2 mitoxantrone resistance-associated protein in normal tissues. *Cancer Lett* **235**:84–92.

Garrett ER and Hunt CA (1974) Physiochemical properties, solubility, and protein binding of delta9-tetrahydrocannabinol. *J Pharm Sci* **63**:1056–1064.

Grotenhermen F (2003) Pharmacokinetics and pharmacodynamics of cannabinoids. *Clin Pharmacokinet* **42**:327–360.

Han LW, Gao C, Zhang Y, Wang J, and Mao Q (2019) Transport of bupropion and its metabolites by the model CHO and HEK293 cell lines. *Drug Metab Lett* **13**:25–36.

Hodges LM, Markova SM, Chinn LW, Gow JM, Kroetz DL, Klein TE, and Altman RB (2011) Very important pharmacogene summary: ABCB1 (MDR1, P-glycoprotein). *Pharmacogenet Genomics* **21**:152–161.

Holland ML, Lau DTT, Allen JD, and Arnold JC (2007) The multidrug transporter ABCG2 (BCRP) is inhibited by plant-derived cannabinoids. *Br J Pharmacol* **152**:815–824.

Karlgren M, Simoff I, Backlund M, Wegler C, Keiser M, Handin N, Müller J, Lundquist P, Jareborg AC, Oswald S, et al. (2017) A CRISPR-Cas9 generated MDCK cell line expressing human MDR1 without endogenous canine MDR1 (cABCB1): an improved tool for drug efflux studies. *J Pharm Sci* **106**:2909–2913.

Loo TW, Bartlett MC, and Clarke DM (2003) Drug binding in human P-glycoprotein causes conformational changes in both nucleotide-binding domains. *J Biol Chem* **278**:1575–1578.

Maliepaard M, Scheffer GL, Faneyte IF, van Gastelen MA, Pijnenborg ACLM, Schinkel AH, van De Vijver MJ, Scheper RJ, and Schellens JHM (2001) Subcellular localization and distribution of the breast cancer resistance protein transporter in normal human tissues. *Cancer Res* **61**:3458–3464.

Mao Q and Unadkat JD (2015) Role of the breast cancer resistance protein (BCRP/ABCG2) in drug transport–an update. *AAPS J* **17**:65–82.

Mi Y and Lou L (2007) ZD6474 reverses multidrug resistance by directly inhibiting the function of P-glycoprotein. *Br J Cancer* **97**:934–940.

Miyake K, Mickley L, Litman T, Zhan Z, Robey R, Cristensen B, Brangi M, Greenberger L, Dean M, Fojo T, et al. (1999) Molecular cloning of cDNAs which are highly overexpressed in mitoxantrone-resistant cells: demonstration of homology to ABC transport genes. *Cancer Res* **59**:8–13.

Patilea-Vrana GI, Anoshchenko O, and Unadkat JD (2019) Hepatic enzymes relevant to the disposition of (2)-Δ^9-tetrahydrocannabinol (THC) and its psychoactive metabolite, 11-OH-THC. *Drug Metab Dispos* **47**:249–256.

Patilea-Vrana GI, and Unadkat JD (2019) Quantifying hepatic enzyme kinetics of (-)-Δ9-tetrahydrocannabinol (THC) and its psychoactive metabolite, 11-OH-THC, through in vitro modeling. *Drug Metab Dispos* **47**:743–752

Qian Y, Gurley BJ, and Markowitz JS (2019) The potential for pharmacokinetic interactions between cannabis products and conventional medications. *J Clin Psychopharmacol* **39**:462–471.

Safar Z, Kis E, Erdo F, Zolnerciks JK, and Krajcsi P (2019) ABCG2/BCRP: variants, transporter interaction profile of substrates and inhibitors. *Expert Opin Drug Metab Toxicol* **15**:313–328.

Schwilke EW, Schwope DM, Karschner EL, Lowe RH, Darwin WD, Kelly DL, Goodwin RS, Gorelick DA, and Huestis MA (2009) Δ9-tetrahydrocannabinol (THC), 11-hydroxy-THC, and 11-nor-9-carboxy-THC plasma pharmacokinetics during and after continuous high-dose oral THC. *Clin Chem* **55**:2180–2189.

Spiro AS, Wong A, Boucher AA, and Arnold JC (2012) Enhanced brain disposition and effects of Δ9-tetrahydrocannabinol in P-glycoprotein and breast cancer resistance protein knockout mice. *PLoS One* **7**:e35937.

Stout SM and Cimino NM (2014) Exogenous cannabinoids as substrates, inhibitors, and inducers of human drug metabolizing enzymes: a systematic review. *Drug Metab Rev* **46**:86–95.

Tournier N, Chevillard L, Megarbane B, Pirnay S, Scherrmann JM, and Declèves X (2010) Interaction of drugs of abuse and maintenance treatments with human P-glycoprotein (ABCB1) and breast cancer resistance protein (ABCG2). *Int J Neuropsychopharmacol* **13**:905–915.

Ueda K, Clark DP, Chen CJ, Roninson IB, Gottesman MM, and Pastan I (1987) The human multidrug resistance (mdr1) gene. cDNA cloning and transcription initiation. *J Biol Chem* **262**:505–508.

US Food and Drug Administration (2020) In vitro drug interaction studies - cytochrome P450 enzyme and transporter mediated drug interactions.

Zhu HJ, Wang JS, Markowitz JS, Donovan JL, Gibson BB, Gefroh HA, and Devane CL (2006) Characterization of P-glycoprotein inhibition by major cannabinoids from marijuana. *J Pharmacol Exp Ther* **317**:850–857.

Address correspondence to: Dr. Qingcheng Mao, Department of Pharmaceutics, School of Pharmacy, University of Washington, Box 357610, Seattle, WA 98195. E-mail: qmao@uw.edu; or Dr. Jashvant D. Unadkat, Department of Pharmaceutics, School of Pharmacy, University of Washington, Box 357610, Seattle, WA 98195. E-mail: jash@uw.edu

Downloaded from dmd.aspetjournals.org at ASPET Journals on October 14, 2022